

Shear viscosity of hot nuclear matter by the mean free path method

D. Q. Fang,^{1,2,3,*} Y. G. Ma,^{1,2,3,4} and C. L. Zhou¹

¹Shanghai Institute of Applied Physics, Chinese Academy of Sciences, Shanghai 201800, China

²Key Laboratory of Nuclear Radiation and Nuclear Energy Technology,
Chinese Academy of Sciences, Shanghai 201800, China

³Kavli Institute for Theoretical Physics, Chinese Academy of Sciences, Beijing 100190, China

⁴Shanghai Tech University, Shanghai 200031, China

(Dated: August 19, 2018)

The shear viscosity of hot nuclear matter is investigated by using the mean free path method within the framework of IQMD model. Finite size nuclear sources at different density and temperature are initialized based on the Fermi-Dirac distribution. The results show that shear viscosity to entropy density ratio decreases with the increase of temperature and tends toward a constant value for $\rho \sim \rho_0$, which is consistent with the previous studies on nuclear matter formed during heavy-ion collisions. At $\rho \sim \frac{1}{2}\rho_0$, a minimum of η/s is seen at around $T = 10$ MeV and a maximum of the multiplicity of intermediate mass fragment (M_{IMF}) is also observed at the same temperature which is an indication of the liquid-gas phase transition.

PACS numbers: 51.20.+d, 51.10.+y, 24.10.-i

Due to van der Waals nature of nuclear force, liquid-gas phase transition (LGPT) occurs in heavy ion collisions (HIC) at energy around hundred MeV/nucleon [1–8]. Studies on the phenomena of LGPT and its probes, like fragment size distribution, caloric curve, bimodality etc., have become the most important subjects in HIC at intermediate energies in the past years [3, 4, 9–12].

Viscosity describes fluid's internal resistance to flow and may be thought of as a measure of fluid friction. In ultra-relativistic HIC, hydrodynamic model has been used to study the Quark Gluon Plasma (QGP) phase and critical phenomenon [13–18]. The investigations show that QGP has very small viscosity over entropy density and behaves like a perfect fluid. A few efforts have also been devoted to the study of viscosity for nuclear matter formed during HIC at intermediate energies [19–28]. It is found that the shear viscosity to entropy density ratio for matter such as H₂O, He and Ne₂ has a minimum at or near the critical point of phase transition [14, 29]. This is an empirical observation for many kinds of substances. A lower bound of this ratio ($\eta/s \geq 1/4\pi$) is speculated to be valid universally according to certain gauge theory (Kovtun-Son-Starinets (KSS) bound) [30, 31]. By using the isospin-dependent quantum molecular dynamics (IQMD) model, we have studied the shear viscosity of finite size hot nuclear matter ($T > 0$) at different densities and also the temperature dependence of η/s . The main purpose of this work is to see whether η/s exhibits a minimum at the temperature of liquid-gas phase transition for nuclear matter.

The quantum molecular dynamics (QMD) model is a many-body theory which describes collisions between two nuclei [32, 33]. Each nucleon i in the nuclei is represented by a Gaussian wave packet with definite width ($L = 2.16$

fm² in the present study) centered around the mean position and the mean momentum. Then the nucleons propagate in the effective nuclear mean field given by

$$U(\rho, \tau_z) = \alpha\left(\frac{\rho}{\rho_0}\right) + \beta\left(\frac{\rho}{\rho_0}\right)^\gamma + \frac{1}{2}(1 - \tau_z)V_c + C_{\text{sym}}\frac{(\rho_n - \rho_p)}{\rho_0}\tau_z + U^{\text{Yuk}}, \quad (1)$$

with the normal nuclear matter density $\rho_0 = 0.16$ fm⁻³. ρ , ρ_n and ρ_p are the total, neutron and proton density, respectively. τ_z is the z -th component of the isospin degree of freedom, which equals 1 for neutron or -1 for proton. The coefficients α , β and γ are parameters for the nuclear equation of state (EOS). $C_{\text{sym}} (= 32$ MeV) is the symmetry energy strength. In the present work, we take $\alpha = -356$ MeV, $\beta = 303$ MeV and $\gamma = 1.17$ which correspond to the so-called soft EOS with the incompressibility of $K = 200$ MeV [32]. V_c is the Coulomb potential and U^{Yuk} is Yukawa (surface) potential. The dynamics of HIC at intermediate energies is governed mainly by three components: the mean field, two-body collisions, and Pauli blocking. Therefore, for an isospin-dependent reaction model, it is important to include isospin degrees of freedom in the above three components. The IQMD model is based on QMD model with consideration of the isospin effects in all these processes [34, 35].

Usually the IQMD model is used to simulate the colliding process between two nuclei. But in the present study, only single nuclear source at $T > 0$ is simulated. The evolution process and thermal properties of this hot nuclear source are studied. The nuclear source with A nucleons is initialized using uniform density distribution with the radius given by $r_0 A^{1/3}$ (r_0 is the radius parameter). Then the initial coordinate of nucleons in the source are obtained by the Monte Carlo sampling method. In the IQMD model, the nucleon radial density can be writ-

*Email: dqfang@sinap.ac.cn

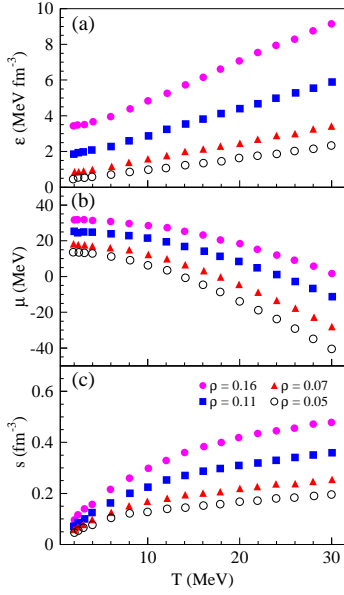


FIG. 1: (Color online) Temperature dependence of energy density (a), chemical potential per nucleon (b) and entropy density (c) for nuclear sources at different densities (the unit of ρ is fm^{-3}).

ten as

$$\rho(r) = \sum_i \frac{1}{(2\pi L)^{3/2}} \exp\left(-\frac{r^2 + r_i^2}{2L}\right) \frac{L}{2rr_i} \times \left[\exp\left(\frac{rr_i}{L}\right) - \exp\left(-\frac{rr_i}{L}\right) \right], \quad (2)$$

with the summation over all nucleons. In the usual QMD study, the initial state of nuclei is in the ground state with $T = 0$. The momentum distribution of nucleon is generated by means of the local Fermi gas approximation with the Fermi momentum calculated by $P_F^i(\vec{r}) = \hbar [3\pi^2 \rho_i(\vec{r})]^{1/3}$, ρ_i is the local density of neutron ($i=n$) or proton ($i=p$). To study hot nuclear source with $T > 0$, the initial momentum distribution of nucleon is determined by the Fermi-Dirac distribution at finite temperature,

$$n(e_k) = \frac{g(e_k)}{e^{\frac{e_k - \mu}{T}} + 1}, \quad (3)$$

where $g(e_k) = \frac{V}{2\pi^2} \left(\frac{2m}{\hbar^2}\right)^{3/2} \sqrt{e_k}$, is the state density for the state with kinetic energy $e_k = \frac{p^2}{2m}$, p is the momentum of nucleon. V is the volume of the source. μ_i is the chemical potential of nucleon which is determined by the following implicit equation

$$\frac{1}{2\pi^2} \left(\frac{2m}{\hbar^2}\right)^{3/2} \int_0^\infty \frac{\sqrt{e_k}}{e^{\frac{e_k - \mu_i}{T}} + 1} de_k = \rho_i. \quad (4)$$

In this work, the nuclear source with 50 protons and 62 neutrons (^{112}Sn) is chosen. The simulated temperature is $0 < T < 30$ MeV. To study the density dependence,

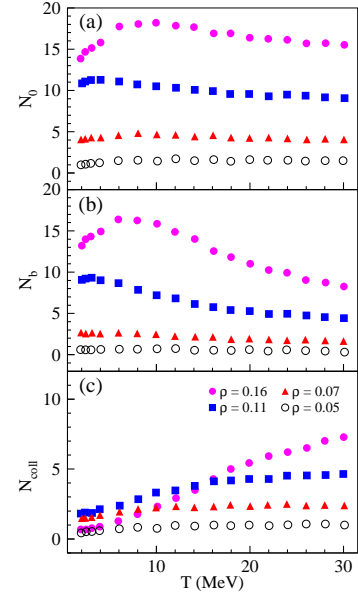


FIG. 2: (Color online) Temperature dependence of the number of possible collision (a), Pauli blocked collision (b) and real collision (c) per fm/c for nuclear sources at different densities. For details see the text.

different radius parameters (r_0) are used to obtain different nuclear densities. The thermal properties could be calculated from the phase space information of the nucleons [24, 36]. The mean kinetic energy density is calculated by

$$\varepsilon = \frac{1}{A} \sum_{i=1}^A e_k^i \rho_i, \quad (5)$$

where e_k^i and ρ_i are the kinetic energy and local density of the i -th nucleon. The mean pressure of the system is calculated by $P = \frac{2}{3}\varepsilon$. The chemical potential of each nucleon is determined by Eq.(4). The entropy density is calculated by

$$s = \frac{\varepsilon + P - \mu\rho}{T}, \quad (6)$$

where μ is the mean chemical potential of the nucleon, ρ is the mean total nucleon density.

In the IQMD model, the temperature and density of the system changes with time when the nucleon propagates in the mean field. The density distribution at any time t could be calculated by Eq.(2), but the exact temperature T at time t is quite difficult to be extracted. To investigate the shear viscosity of nuclear matter at definite temperature and density, thermal properties and η are extracted from the phase space of nucleons at the very early time ($1 < t < 5$ fm/c). During this period of time, the temperature of the system is almost the same as the initial value which is given by input. In Fig. 1(a)-(c), the temperature dependence of energy density, chemical potential per nucleon and entropy density are shown. As

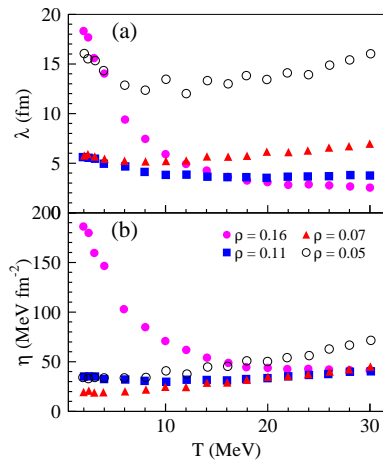


FIG. 3: (Color online) Temperature dependence of the mean free path (a) and the shear viscosity (b) for nuclear sources at different densities.

expected, the energy density increases with T . Since the nuclear source studied is almost symmetric, the mean chemical potential of neutron and proton is presented in the figure. μ is close to the Fermi energy when T is close to 0. Due to the Fermi-Dirac distribution for the momentum of nucleon, μ decreases with the increase of T which makes more particles occupy high energy states. The entropy density increases with T , indicating that the system becomes more disorder with the increase of temperature. The energy density, chemical potential and entropy density are proportional to the nuclear density as shown in the three panels.

In Refs. [24, 25], we have studied η of nuclear matter formed during HIC processes using the Green-Kubo formula which employs the linear-response theory to relate the transport coefficients as correlations of dissipative fluxes [37] and also a parameterized function by P. Danielewicz [20, 26]. On the other hand, the classical kinetic theory relates η of the system with the mean free path of the particle. In the kinetic theory [38],

$$\eta = \frac{1}{3}\rho m v \lambda, \quad (7)$$

where ρ , m and v are the density, mass and velocity of the nucleon. λ is the mean free path of nucleon which can be determined by

$$\lambda = \frac{A}{2N_{\text{coll}}}v, \quad (8)$$

with N_{coll} being the collision number per fm/c (or collision frequency).

The possible collision, Pauli blocked collision and real collision numbers per fm/c against temperature are shown in Fig. 2. The possible collisions (N_0) in the IQMD simulation is determined directly by the nucleon-nucleon cross section. Among these collisions, some collisions will really happen but some collisions will not happen at all.

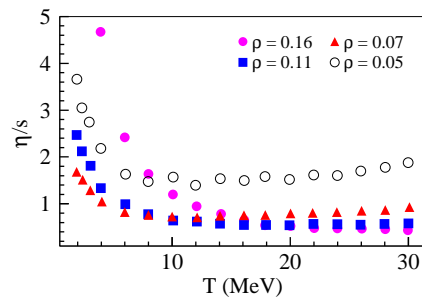


FIG. 4: (Color online) Temperature dependence of η/s for nuclear sources at different densities.

The collision not happened is the Pauli blocked collision (N_b). While the real happened collision is denoted by N_{coll} . From the definition, we have $N_{\text{coll}} = N_0 - N_b$. At low temperature, the Pauli blocking effect is large due to the small phase space (momentum space), especially in the high density case. At high temperature, nucleon can occupy high momentum state which increases the phase space of the system. In this case, the Pauli blocking effect decreases. The effect of Pauli blocking is clearly seen from Fig. 2(a)-(c), which will greatly affect the mean free path of nucleon and also the shear viscosity, especially at low temperature. The obtained mean free path is given in Fig. 3 (a). When the density is fixed, the mean free path is proportional to the velocity (temperature) but inversely proportional to the collision frequency. At high density like $\rho = 0.16 \text{ fm}^{-3}$, the collision frequency increases very quickly with the temperature. The mean free path decreases with T even though the velocity increases with the temperature. While at low density like $\rho = 0.05 \text{ fm}^{-3}$, the collision frequency is almost constant in comparison with the high density case, thus the mean free path increases with T . For the other two densities, the decrease of collision frequency and increase of velocity is comparable, so the mean free path doesn't change too much with the increase of T .

The shear viscosity is shown in Fig. 3 (b). At density $\rho = 0.16 \text{ fm}^{-3}$, η decreases with T and is saturated to a value around 50 MeV fm^{-2} that is similar to the parameterized formula of $\eta(T)$ [20] as well as the Green-Kubo method [25]. At low densities, η decrease with T first but increase with T when T is larger than $8 \sim 10 \text{ MeV}$.

η/s is shown in Fig. 4. At densities $\rho = 0.16, 0.11 \text{ fm}^{-3}$, η/s decreases with the increase of T and becomes saturated to a value round 0.75 (about 7 – 8 times of KSS bound) when $T > 20 \text{ MeV}$. But at low densities of $\rho = 0.07$ and 0.05 fm^{-3} , a minimum is seen at around 10 MeV . From the general relation between η/s and T , this minimum might have connection with the liquid-gas phase transition point of nuclear matter. In order to check this conclusion, multiplicity of intermediate mass fragment (IMF) is investigated since it is a widely studied observable for LGPT.

To obtain the fragment distribution, evolution of the hot nuclear source is studied. After the initialization,

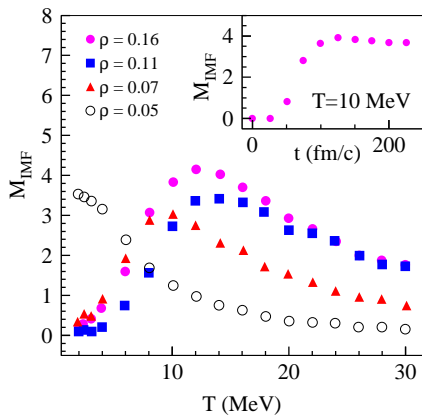


FIG. 5: (Color online) Temperature dependence of the multiplicity of IMF (M_{IMF}) after the freeze-out of the system for nuclear sources at different densities. Inset is the time evolution of M_{IMF} at $T = 10$ MeV for $\rho = 0.16$ fm $^{-3}$. For details see the text.

the nucleons propagate in the mean field with no boundary condition. It means that the system will expand and freeze-out by emitting nucleon and fragments. The nuclear fragments are constructed by using the coalescence model, in which nucleons with relative momentum smaller than 300 MeV/c and relative distance smaller than 3.5 fm will be combined into a cluster. A fragment with its charge number (Z) fulfilling $3 \leq Z \leq Z_{\text{src}}$ is defined as IMF, where Z_{src} is the charge number of the nuclear source. From the time evolution of the fragment distribution, it is found that the yields of each fragment become stable after 100 fm/c for almost all temperature T . It indicates that the system is freeze-out after this time as shown by the time dependence of the multiplicity of IMF (M_{IMF}) at $T = 10$ MeV in the inset of Fig. 5. M_{IMF} against T at 150 fm/c is shown in Fig. 5. At $\rho = 0.07$ fm $^{-3}$, a maximum of M_{IMF} is seen at 10 MeV which is almost the same as the temperature of the minimum of η/s at this density as shown in Fig. 4. This result indicates that η/s has a minimum value at $T \sim 10$

MeV when the density is around $\frac{1}{2}\rho_0$. At the same temperature, M_{IMF} of the system after freeze-out takes a maximum value which is the signal of liquid-gas phase transition [39]. The phase transition temperature is consistent with other studies [5, 40]. While for higher densities $\rho = 0.16, 0.11$ fm $^{-3}$, no minimum of η/s is seen but instead η/s approaches to an asymptotical value at higher temperature. However, the maximum of M_{IMF} is at $T \sim 12$ MeV. Since no boundary condition is used in the present calculation, the density of the system will change with time quickly, especially for the source at high density. For low density $\rho = 0.05$ fm $^{-3}$, the initial distance between nucleons is large and the system will be easy to form a gas state at $T > 0$ with no boundary condition, so the maximum of M_{IMF} is close to $T = 0$. Thus it will be very interesting to study η and η/s for infinite uniform nuclear matter. In this case, η/s and M_{IMF} will be obtained at the same density condition.

In summary, we have studied the shear viscosity of hot nuclear sources with $0 < T < 30$ MeV at different densities. η is calculated by the mean free path method in which the nucleon-nucleon collision number per fm/c plays an important role. The absolute value of η and its temperature dependence is consistent with the previous studies. At $\rho \sim \frac{1}{2}\rho_0$, a minimum of η/s is seen at around 10 MeV and a maximum of M_{IMF} is also observed at the same temperature which is the indication of the liquid-gas phase transition. Thus a minimum of η/s is observed at the location of the liquid-gas phase transition for $\rho \sim \frac{1}{2}\rho_0$, which is in accordance with the general phenomenon observed for other matter. To fully understand the relation between η/s and liquid-gas phase transition, further investigations on η and η/s for infinite uniform nuclear matter are expected.

This work is supported by the Major State Basic Research Development Program of China under contract No. 2013CB834405, National Natural Science Foundation of China under contract No.s 11175231 and 11035009, and Knowledge Innovation Project of CAS under Grant No. KJCX2-EW-N01.

-
- [1] D. H. E. Gross, Rep. Prog. Phys. **53**, 605 (1990).
 - [2] J. P. Bondorf *et al.*, Phys. Rep. **257**, 133 (1995).
 - [3] J. Pochodzalla *et al.* (ALADIN Collaboration), Phys. Rev. Lett. **75**, 1040 (1995).
 - [4] Y. G. Ma, Phys. Rev. Lett. **83**, 3617 (1999); Eur. Phys. J. A **6**, 367 (1999).
 - [5] J. B. Natowitz *et al.*, Phys. Rev. Lett. **89**, 212701 (2002).
 - [6] S. Das Gupta, A. Z. Mekjian, and M. B. Tsang, Adv. Nucl. Phys. **26**, 89 (2001).
 - [7] B. Borderie, M. F. Rivet, Progr. Part. Nucl. Phys. **61**, 551 (2008).
 - [8] M. Veselsky and Y. G. Ma, Phys. Rev. C **87**, 034615 (2013).
 - [9] M. E. Fisher, Rep. Prog. Phys. **30**, 615 (1969); Physics **3**, 255 (1967).
 - [10] F. Gulminelli and M. D'Agostino, Eur. Phys. J. A **30**, 253 (2006).
 - [11] O. Lopez and M.F. Rivet, Eur. Phys. J. A **30**, 263 (2006).
 - [12] Y. G. Ma *et al.*, Phys. Rev. C **71**, 054606 (2005).
 - [13] N. Demir and S. A. Bass, Phys. Rev. Lett. **102**, 172302 (2009).
 - [14] R. Lacey *et al.*, Phys. Rev. Lett. **98**, 092301 (2007).
 - [15] J. W. Chen and E. Nakano, Phys. Lett. B **647**, 371 (2007).
 - [16] J. I. Kapusta and T. Springer, Phys. Rev. D **78**, 066017 (2008).
 - [17] A. Majumder, B. Müller, X. N. Wang, Phys. Rev. Lett. **99**, 192301 (2007).
 - [18] J. Noronha-Hostler, J. Noronha and C. Greiner, Phys. Rev. Lett. **103**, 172302 (2009).

- [19] J. W. Chen, Y. H. Li, Y. F. Liu and E. Nakano, Phys. Rev. D **76**, 114011 (2007).
- [20] P. Danielewicz, Phys. Lett. B **146**, 168 (1984).
- [21] L. Shi and P. Danielewicz, Phys. Rev. C **68**, 064604 (2003).
- [22] S. Pal, Phys. Lett. B **684**, 211 (2010); Phys. Rev. C **81**, 051601(R) (2010).
- [23] N. Auerbach and S. Shlomo, Phys. Rev. Lett. **103**, 172501 (2009).
- [24] S. X. Li, D. Q. Fang, Y. G. Ma, C. L. Zhou, Phys. Rev. C **84**, 024607 (2011); Nucl. Sci. Tech. **22**, 235 (2011).
- [25] C. L. Zhou *et al.*, Euro. Phys. Lett. **98**, 66003 (2012).
- [26] C. L. Zhou, Y. G. Ma, D. Q. Fang, G. Q. Zhang, Phys. Rev. C **88**, 024604 (2013).
- [27] J. Xu, Nucl. Sci. Tech. **24**, 050514 (2013); J. Xu, Phys. Rev. C **84**, 064603 (2011).
- [28] J. Xu *et al.*, Phys. Lett. B **727**, 244 (2013).
- [29] L. P. Csernai, J. I. Kapusta and L. D. McLerran, Phys. Rev. Lett. **97**, 152303 (2006).
- [30] P. K. Kovtun, D. T. Son and A. O. Starinets, Phys. Rev. Lett. **94**, 111601 (2005).
- [31] G. Policastro, D. T. Son and A. O. Starinets, Phys. Rev. Lett. **87**, 081601 (2001).
- [32] J. Aichelin, Phys. Rep. **202**, 233 (1991).
- [33] C. Hartnack *et al.*, Eur. Phys. J. A **1**, 151 (1998).
- [34] X. G. Cao *et al.*, Phys. Rev. C **86**, 044620 (2012); J. Wang *et al.*, Nucl. Sci. Tech. **24**, 030501 (2013).
- [35] C. Tao, Y. G. Ma *et al.*, Phys. Rev. C **87**, 014621 (2013); Nucl. Sci. Tech. **24**, 030502 (2013).
- [36] A. Muronga, Phys. Rev. C **69**, 044901 (2004).
- [37] R. Kubo, Rep. Prog. Phys. **29**, 255 (1966).
- [38] K. Huang, Statistical Mechanics, 2nd ed. (John Wiley & Sons, New York, 1987).
- [39] Y. G. Ma and W. Q. Shen, Phys. Rev. C **51**, 710 (1995).
- [40] H. Q. Song and R. K. Su, Phys. Rev. C **44**, 2505 (1991).